Supporting Information of

General Thermal Texturization Process of MoS_2 for Efficient Electrocatalytic Hydrogen Evolution Reaction

*Daisuke Kiriya,[1,3,4]‡ Peter Lobaccaro,[2,4,5]‡ Hnin Yin Yin Nyein,[1,3,4] Peyman Taheri,[1,4] Mark Hettick,[1,3,4,5] Hiroshi Shiraki,[1,3,4] Carolin M. Sutter-Fella,[1,3,4] Peida Zhao,[1,3,4] Wei Gao,[1,3,4] Roya Maboudian,[2,4] Joel W. Ager,[3,5] and Ali Javey[1,3,4]**

[1] Department of Electrical Engineering and Computer Sciences, University of California at Berkeley, Berkeley, California 94720, United States

[2] Department of Chemical and Biomolecular Engineering, University of California at Berkeley, Berkeley, California 94720, United States

[3] Materials Sciences Division, Lawrence Berkeley National Laboratory, Berkeley, California 94720, United States

[4] Berkeley Sensor & Actuator Center, University of California, Berkeley, California 94720, United States

[5] Joint Center for Artificial Photosynthesis, Lawrence Berkeley National Laboratory, Berkeley, California 94720, United States

‡ These authors contributed equally for this paper.

*** Corresponding Author:**

Prof. Ali Javey

E-mail: ajavey@berkeley.edu

Experimental Methods

Sample preparation

Bulk mineral MoS_2 was purchased from SPI Supplies. Micron-scale (microflake) MoS_2 was purchased from Graphene Supermarket. Some microflake MoS_2 was further prepared by grinding it with a mortar and pestle in an attempt to make smaller flakes. This material is called ground microflake. Microflake and ground microflake films were prepared by the following process: 1) Disperse the flakes in DMF at a concentration of 30 mg/ml via sonication. 2) Cast the suspension (~100 μL) on a 1 cm × 1.5 cm Mo foil on a hotplate at 120 °C. After drying off the DMF solvent (about 5 min), repeat the suspension casting again. All samples termed as-received MoS_2 (bulk and microflake film) or as-ground (ground microflake film) underwent a 250 ^{o}C forming gas anneal for 3 hrs to clean the surface and remove any remaining DMF solvent. This temperature has essentially no effect on MoS_2. High temperature annealed samples were annealed at 700 °C, 800 ^{o}C, or 900 °C in forming gas for 3 hrs. The samples were allowed to cool below 50 ^{o}C before being taken out of the annealing chamber.

HER measurement

Bulk mineral MoS_2 samples needed to be mounted before they could be used as electrodes. Silver paste (CircuitWorks) was used to mount the flakes to a glass slide. The stack was then annealed at 70 °C in air to cure the Ag paste. Then Cu tape was placed on the edge of the Ag paste to make an electrical lead connection. Finally, insulating, acid-resistant, polymer resin was painted over the entire area except for the desired MoS_2 area identified for measurement. For the microflake and ground microflake film samples, the same resin was used to cover the whole area of the film except for the identified measurement area. These samples were placed as working electrode in the 3-electrode cell as shown in **Figure 4a**.

The HER measurements were done in 0.5 M H_2SO_4 (Sigma-Aldrich) with a calibrated Ag/AgCl reference electrode and a platinum counter electrode. The electrolyte was initially sparged with N_2

bubbling for more than 10 mins to remove oxygen. N_2 was then flown over the headspace of the electrolyte during the measurements. The electrolyte was constantly stirred at 750 RPM with a magnetic, Teflon coated, stir bar. A Biologic SP-300 potentiostat was used to make all electrochemical measurements. IR drop was corrected for during the CV measurements by first running electrochemical impedance spectroscopy from 10^6 to 1000 Hz to identify the resistivity. This resistance was found to be typically less than 10 Ohms. Cyclic voltammetry was used at two different scan rates to obtain the data for the Tafel plots (5 mV/sec) and polarization curves (50 mV s^{-1}).

Electrochemical Active Surface Area (ECSA) Measurement

To identify the electrochemically active surface areas to normalize the polarization curves as shown in Figure 4d, ECSA measurements were used. Bulk MoS_2 (as-received and annealed samples) were mounted as stated to be used as the working electrode in the three electrode setup shown in Figure 4a. We employed electrochemical impedance spectroscopy, using a Biologic SP-300 potentiostat, at open circuit potential scanning frequencies from 10 Hz to ~0.05 Hz. Then a R-C equivalent circuit was used to fit the data to determine the double-layer capacitance of each sample. The double layer capacitances were obtained as the follows: As-received, ~ 4.14 μF cm^{-2}; 700 °C annealed sample, ~ 0.47 μF cm^{-2}; 800 °C annealed sample, ~ 2.95 μF cm^{-2}; 900 °C annealed sample, ~ 2.83 μF cm^{-2}. The relative active surface areas are obtained from the relative values of the above double layer capacitances. Using these values, the currents (mA) were normalized as shown in Figure 4d.

Characterization

SEM images were obtained with either a FEI Quanta 200 FEG SEM with an operating voltage of 15 kV (Figures 2, 3, 5, 6, and S6) or with a FEI Nova NanoSEM650 with an operating voltage of 5 kV (Figures S3 and S4). XPS characterization was performed using a Kratos Axis Ultra DLD system using a monochromatic Al Kα source ($h\nu$ = 1486.6 eV). The XRD patterns were taken on a Rigaku SmartLab

system which is capable of measuring both grazing incidence and normal XRD patterns. TEM images were taken with a FEI Titan microscope with an operating voltage at 200 kV.

Tafel Analysis

To attempt to understand the HER mechanism for the samples, the Tafel plots were examined. The Tafel equation ($\eta = b*\log j + a$, where η is overpotential, j is the current density, b is the Tafel slope, and a is the Tafel constant) was applied to make Tafel plots of Log(j) vs. η and the Tafel slope, b, was obtained. All the measurements for this analysis were carried out with 5 mV sec^{-1} scan rates. The obtained Tafel slopes for the samples are shown in **Table S1**.

The three possible reaction mechanisms for HER in acidic media are known as the Volmer, the Heyrovsky, and the Tafel reactions[1,2]:

Volmer step: $H_3O^+ + e^- \rightarrow H_{ads} + H_2O$

Heyrovsky step: $H_{ads} + H_3O^+ + e^- \rightarrow H_2 + H_2O$

Tafel step: $H_{ads} + H_{ads} \rightarrow H_2$

If the rate determining step in HER is one of the above reactions, the Tafel slope should be close to either ~120 mV $decade^{-1}$, ~40 mV $decade^{-1}$, or ~30 mV $decade^{-1}$ for the Volmer, the Heyrovsky, or the Tafel reaction respectively. According to the above considerations, the rate determining step for the as-received bulk MoS_2 is suggested to be the Volmer reaction (Tafel slope ~150 mV $decade^{-1}$) and the annealed bulk MoS_2 samples could possibly be the Heyrovsky reaction (Tafel slope ~60 mV $decade^{-1}$). The exchange current density (j_0) is also an important parameter which indicates the inherent catalytic activity of the material. The exchange current density was calculated from the Tafel plot and is also shown in **Table S1**.

Table S1. Electrochemical parameters for bulk mineral, microflake, ground microflake and sprayed nanoflake films of MoS_2.

Morphology	Annealing Temp. (°C)	Overpotential (mV) at j = 10 mA cm^{-2}	j_0 (mA cm^{-2})	Tafel slope (mV decade^{-1})
Bulk mineral	250*	–**	0.00093	149
Bulk mineral	700	–**	0.0011	90
Bulk mineral	800	300	0.00069	71
Bulk mineral	900	296	0.0012	76
Microflake	250*	330	0.00012	63
Microflake	700	227	0.0044	67
Microflake	800	210	0.0048	63
Microflake	900	195	0.0045	59
Ground microflake	250*	342	0.00046	73
Ground microflake	700	220	0.0093	70
Ground microflake	800	193	0.011	64
Ground microflake	900	174	0.019	63
Sprayed nanoflake	250*	322	0.0030	92
Sprayed nanoflake	700	215	0.0038	62

* The samples are referred to as as-received or as-ground in the manuscript. Annealing at 250 °C does not damage MoS_2 flakes.

** Not observed in the measurement range.

Table S2. Comparison of electrical parameters with other reported works. Data adapted from Benck et al.[3]

Catalyst Description	Overpotential (mV) at j = 10 mA cm^{-2}	Reference
Amorphous MoS_x on n-doped carbon nanotubes	110	Li 2014[4]
Li^+ intercalated MoS_2 nanoparticles on carbon fiber	110	Wang 2014[5]
$[Mo_3S_{13}]^{-2}$ loaded on anodized Toray paper	149	Benck 2014[3]
MoS_x loaded on carbon fiber	152	Laursen 2013[6]
MoS_2 nanoparticles on reduced graphene oxide	154	Li 2011[1]
Li^+ intercalated MoS_2	168	Wang 2013[7]
100 µg/cm^2 $[Mo_3S_{13}]^{-2}$ loaded on Toray paper	174	Kibsgaard 2014[8]
MoS_x loaded on carbon fiber paper	194	Laursen 2013[6]
Wet chemical synthesized amorphous MoS_2	200	Benck 2012[9]
Double gyroid morphology MoS_2	206	Kibsgaard 2012[10]
1-T phase MoS_2	207	Voiry 2013[11]
Electrodeposited amorphous MoS_2	242	Merki 2011[12]
$MoO_3 – MoS_2$ NWs	254	Chen 2011[13]
Thermally texturized ground microflake MoS_2	174	This work

Supporting Figures

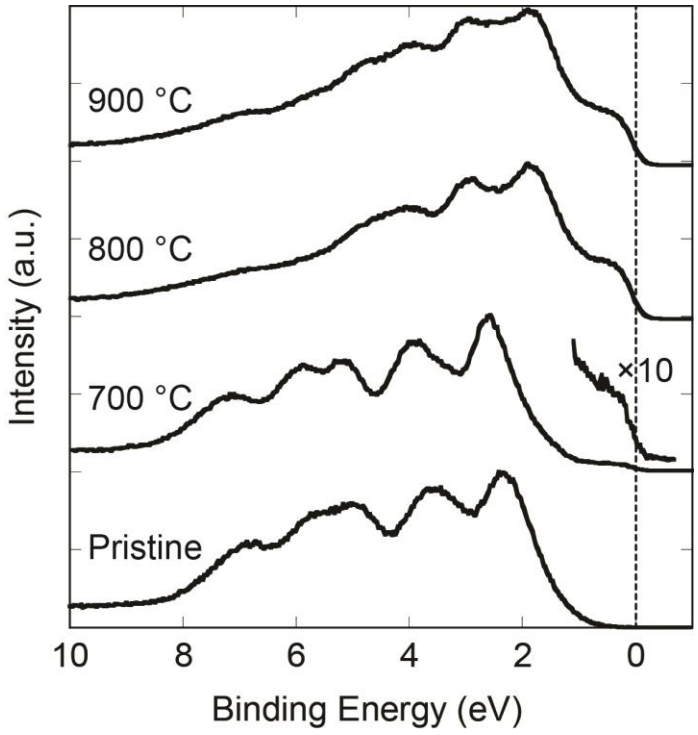

Figure S1. XPS spectra around the valence band region of the bulk mineral MoS_2 of pristine (annealed at 250 °C for 3hrs) and annealed at 700 °C to 900 °C for 3 hrs.

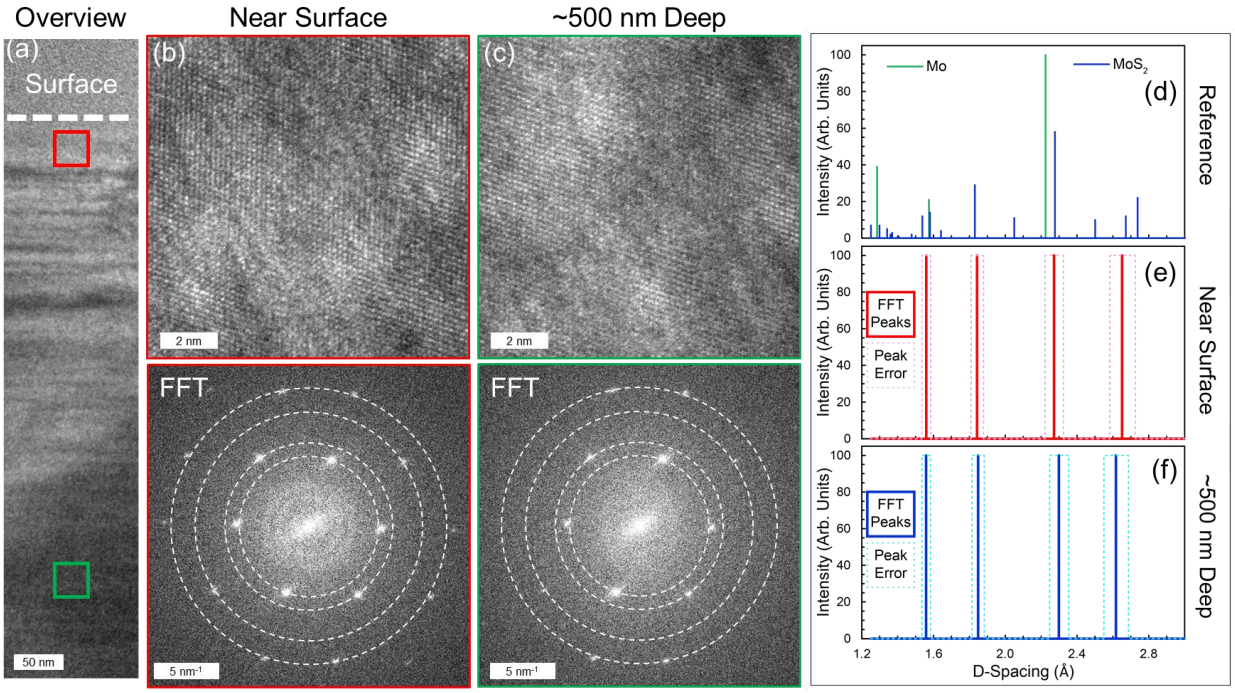

Figure S2. The structure of a thermally texturized sample at 700 °C (3 hrs annealing) was investigated using cross-sectional TEM. (a) Low resolution TEM image of the sample. (b,c) High-resolution TEM images near the surface approximately ~25 nm (b) and deeper inside the sample, approximately 500 nm from the surface (c). Fast Fourier transform (FFT) of these images are shown below. (d-f) D-spacings were obtained from the FFT patterns in Figure S2b and c and other images not shown here. (d) Reference powder XRD patterns of MoS_2 and Mo, compared to D-spacing patterns obtained from the FFT analysis for the near surface region (e) and for the deeper region (f). FFT peaks (solid line) and errors (dot line) are shown in the plot.

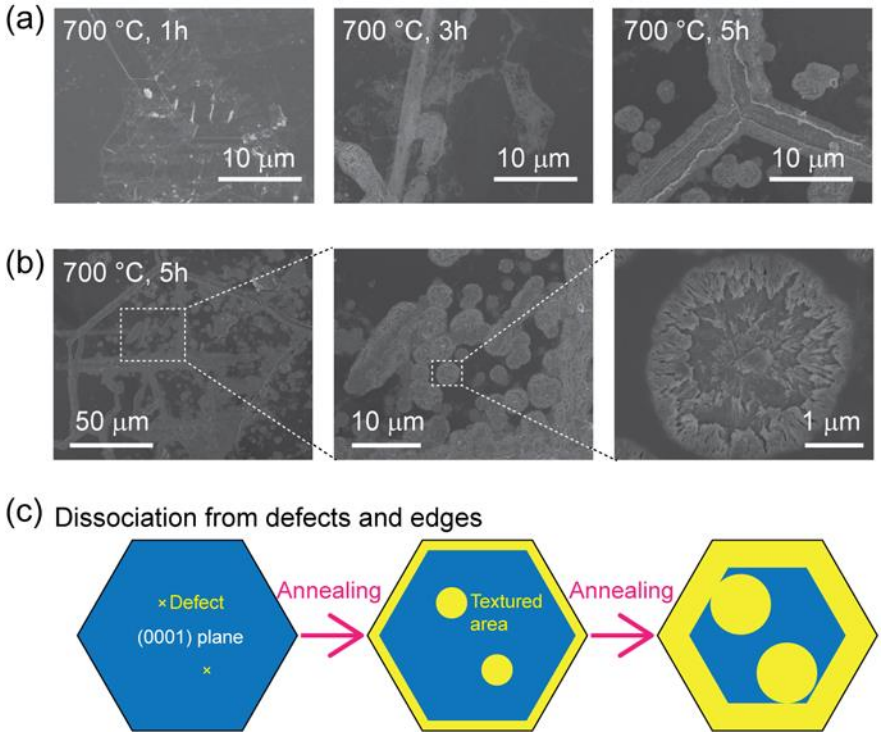

Figure S3. Mechanism of the thermal texturization process which occurs on the MoS_2 surface under a forming gas environment (H_2/N_2 = 5%/95%). (a) SEM images of the bulk mineral MoS_2 annealed at 700 °C for different annealing times (1h to 5 hrs). The light gray areas are dissociatively textured by the thermal annealing processes. Annealing longer than 3 hrs shows clear dissociation under SEM. (b) The detailed surface morphology for the bulk MoS_2 annealed at 700 °C for 5 hrs. The surface texturization is observed as either lines or circles. The circles are radially grown, indicating the dissociation occurs from a defect at the center. (c) A plausible mechanism for the thermal texturization process is shown. The texture would emanate from defects and edges on the surface.

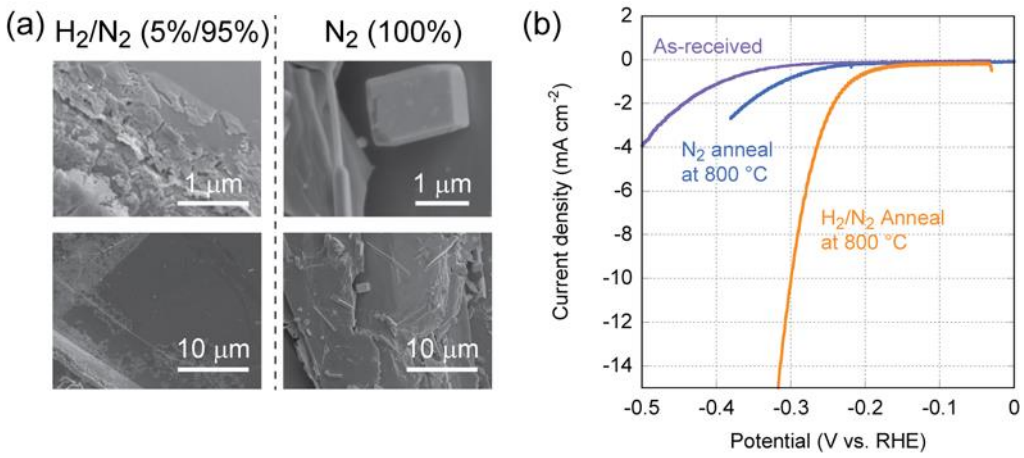

Figure S4. Environmental effect of the annealing process on bulk mineral MoS_2. (a) SEM images of the annealed bulk MoS_2 in forming gas (left) and nitrogen (right) at 800 °C for 3 hrs. In the forming gas anneal case, the dissociation causes texturization of the surface. On the other hand, in the nitrogen anneal case, the surface is still smooth even after annealing at 800 °C and large cubic structures are observed. (b) Polarization curves for the HER activity of as-received bulk MoS_2, 800 °C annealed bulk MoS_2 under nitrogen, and 800 °C annealed bulk MoS_2 under forming gas are shown. The nitrogen annealed sample shows much lower HER performance than the sample annealed in forming gas.

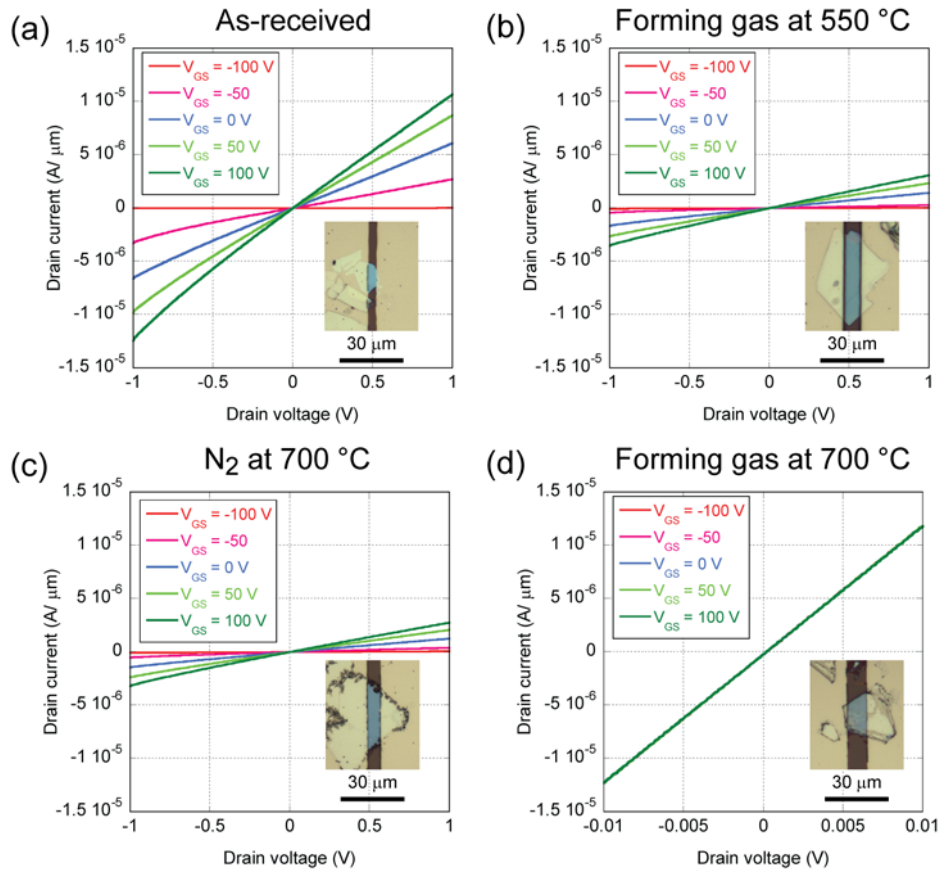

Figure S5. The output characteristic curves for the MOSFETs of (a) as-received bulk MoS_2, (b) annealed bulk MoS_2 at 550 °C in forming gas, (c) annealed bulk MoS_2 at 700 °C in nitrogen, and (d) annealed bulk MoS_2 at 700 °C in forming gas. These samples are annealed at their respective temperatures for 3 hrs. MoS_2 flakes (thickness of ~100 nm) were prepared by a mechanical exfoliation technique, then annealed at the aforementioned temperatures followed by a typical lithography process to make the devices. The channel length was fixed at 10 µm in all cases. Back gate potential was applied from -100 V to 100 V. Except for the forming gas 700 °C annealed sample, all samples showed gate dependency, indicating semiconducting n-type MoS_2. The characteristics curve in Figure S5d shows a sample with no gate dependency, indicating metallic behavior of the MoS_2 flake after the thermal texturization process.

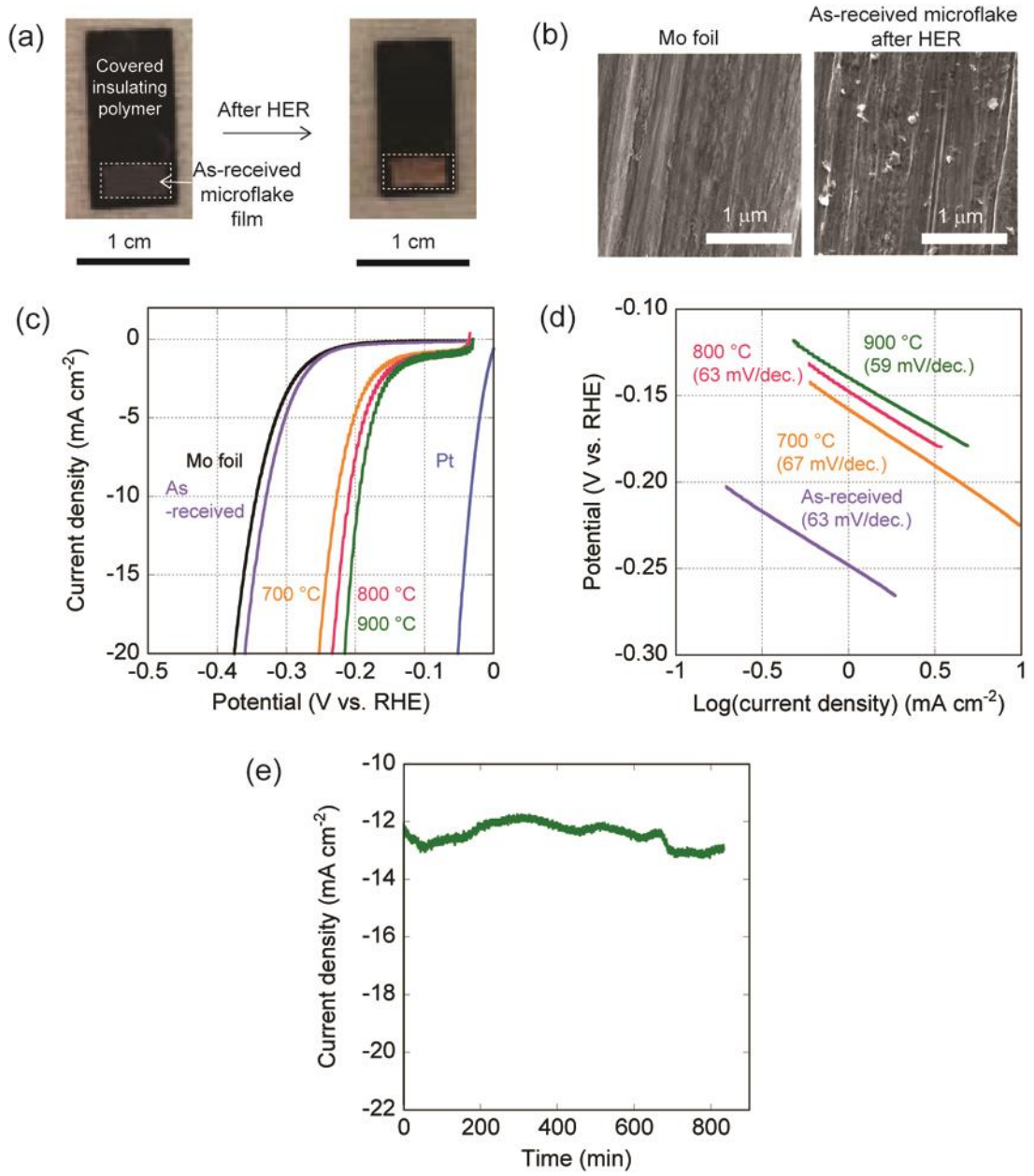

Figure S6. (a) Macroscopic images for the as-received microflake MoS_2 films (annealed at 250 °C for 3 hrs) on Mo foil as the working electrode before (left) and after (right) HER in 0.5 M H_2SO_4. The area exposed during electrolysis was completely delaminated by the generation of hydrogen bubbles. (b) SEM images of Mo foil (left) and the surface of the as-received microflake MoS_2 film after delamination (right). Small amounts of MoS_2 flakes remained on the Mo foil after the delamination. (c) Polarization curves (50 mV s^{-1}) in 0.5 M H_2SO_4 for the microflake MoS_2 samples annealed at different temperatures, including Mo and Pt foils for reference. (d) Tafel plot of the samples shown in Figure S6c

taken at 5mV s^{-1}. (e) Chronoamperometric curve (*j*-*t*) measured for a microflake MoS_2 film annealed at 900 °C for 13hrs.

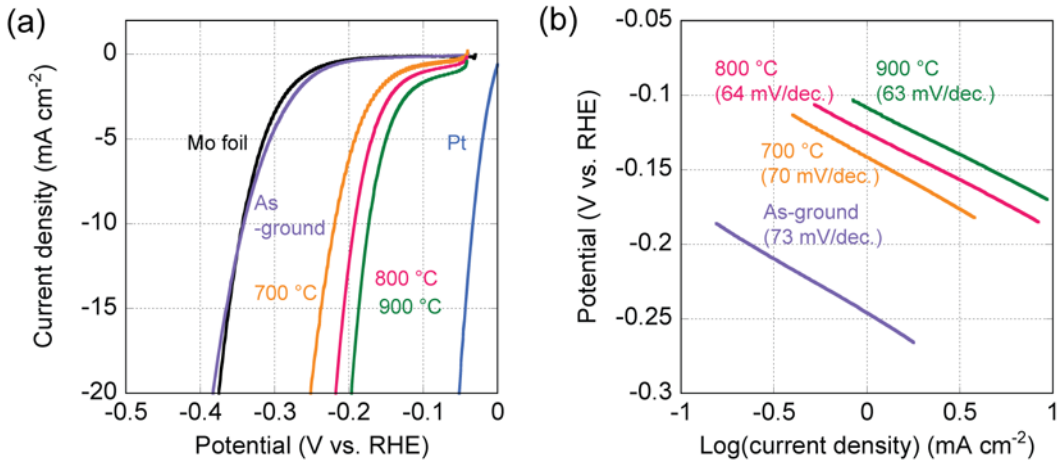

Figure S7. (a) Polarization curves (50 mV s^{-1}) in 0.5 M H_2SO_4 for the ground microflake MoS_2 samples annealed at different temperatures, including Mo and Pt foils for reference. The as-ground MoS_2 film delaminated after evolving hydrogen similar to what is shown in Figure S6a, resulting in the observed activity matching closely to Mo foil. (b) Tafel plot of the samples shown in Figure S7a taken at 5 mV s^{-1}.

Supporting References

(1) Li, Y.; Wang, H.; Xie, L.; Liang, Y.; Hong, G.; Dai, H. *J. Am. Chem. Soc.* **2011**, *133*, 7296–7299.

(2) Conway, B. E.; Tilak, B. V. *Electrochim. Acta,* **2002**, *47*, 3571–3594.

(3) Benck, J. D.; Hellstern, T. R.; Kibsgaard, J.; Chakthranont, P.; Jaramillo, T. F. *ACS Catal.* **2014**, *4*, 3957–3971.

(4) Li, D. J.; Maiti, U. N.; Lim, J.; Choi, D. S.; Lee, W. J.; Oh, Y.; Lee, G. Y.; Kim, S. O. *Nano Lett.* **2014**, *14*, 1228–1233.

(5) Wang, H.; Lu, Z.; Kong, D.; Sun, J.; Hymel, T. M.; Cui, Y. *ACS Nano* **2014**, *8*, 4940–4947.

(6) Laursen, A. B.; Vesborg, P. C. K.; Chorkendorff, I. *Chem. Commun.* **2013**, *49*, 4965.

(7) Wang, H.; Lu, Z.; Xu, S.; Kong, D.; Cha, J. J.; Zheng, G.; Hsu, P.-C.; Yan, K.; Bradshaw, D.; Prinz, F. B.; Cui, Y. *Proc. Natl. Acad. Sci.* **2013**, *110*, 19701–19706.

(8) Kibsgaard, J.; Jaramillo, T. F.; Besenbacher, F. *Nat. Chem.* **2014**, *6*, 248–253.

(9) Benck, J. D.; Chen, Z.; Kuritzky, L. Y.; Forman, A. J.; Jaramillo, T. F. *ACS Catal.* **2012**, *2*, 1916–1923.

(10) Kibsgaard, J.; Chen, Z.; Reinecke, B. N.; Jaramillo, T. F. *Nat. Mater.* **2012**, *11*, 963–969.

(11) Voiry, D.; Salehi, M.; Silva, R.; Fujita, T.; Chen, M.; Asefa, T.; Shenoy, V. B.; Eda, G.; Chhowalla, M. *Nano Lett.* **2013**, *13*, 6222–6227.

(12) Merki, D.; Fierro, S.; Vrubel, H.; Hu, X. *Chem. Sci.* **2011**, *2*, 1262–1267.

(13) Chen, Z.; Cummins, D.; Reinecke, B. N.; Clark, E.; Sunkara, M. K.; Jaramillo, T. F. *Nano Lett.* **2011**, *11*, 4168–4175.